Evidence for environment-dependent galaxy Luminosity Function up to $z = 1.5$ in the VIMOS-VLT Deep Survey[⋆]

O. Ilbert[1], O. Cucciati[2], C. Marinoni[3,4], L. Tresse[4], O. Le Fèvre[4], G. Zamorani[5], S. Bardelli[5], A. Iovino[2], E. Zucca[5], S. Arnouts[4], D. Bottini[6], B. Garilli[6], V. Le Brun[4], D. Maccagni[6], J.P. Picat[8], R. Scaramella[12], M. Scodeggio[6], G. Vettolani[7], A. Zanichelli[7], C. Adami[4], M. Bolzonella[1], A. Cappi[5], S. Charlot[11], P. Ciliegi[5], T. Contini[8], S. Foucaud[6], P. Franzetti[6], I. Gavignaud[8,13], L. Guzzo[2], B. Marano[1], A. Mazure[4], H.J. McCracken[11], B. Meneux[6], R. Merighi[5], S. Paltani[14,15], R. Pellò[8], A. Pollo[4], L. Pozzetti[5], M. Radovich[9], M. Bondi[7], A. Bongiorno[1], G. Busarello[9], S. De La Torre[4], L. Gregorini[10], F. Lamareille[8], G. Mathez[8], Y. Mellier[11,16], P. Merluzzi[9], V. Ripepi[9], D. Rizzo[8], and D. Vergani[6]

[1] Università di Bologna, Dipartimento di Astronomia - Via Ranzani 1, 40127, Bologna, Italy
[2] INAF-Osservatorio Astronomico di Brera - Via Brera 28, Milan, Italy
[3] Centre de Physique Théorique, Marseille, France
[4] Laboratoire d'Astrophysique de Marseille, UMR 6110 CNRS-Université de Provence, BP8, 13376 Marseille Cedex 12, France
[5] INAF-Osservatorio Astronomico di Bologna - Via Ranzani 1, 40127, Bologna, Italy
[6] IASF-INAF - via Bassini 15, 20133, Milano, Italy
[7] IRA-INAF - Via Gobetti,101, 40129, Bologna, Italy
[8] Laboratoire d'Astrophysique de l'Observatoire Midi-Pyrénées, UMR 5572, 14 avenue E. Belin, 31400 Toulouse, France
[9] INAF-Osservatorio Astronomico di Capodimonte - Via Moiariello 16, 80131, Napoli, Italy
[10] INAF-Osservatorio Astronomico di Brera - Via Brera 28, Milan, Italy
[11] Institut d'Astrophysique de Paris, UMR 7095, 98 bis Bvd Arago, 75014 Paris, France
[12] INAF-Osservatorio Astronomico di Roma - Via di Frascati 33, 00040, Monte Porzio Catone, Italy
[13] European Southern Observatory, Garching, Germany
[14] Integral Science Data Centre, ch. d'Écogia 16, CH-1290 Versoix
[15] Geneva Observatory, ch. des Maillettes 51, CH-1290 Sauverny
[16] Observatoire de Paris, LERMA, 61 Avenue de l'Observatoire, 75014 Paris, France

Abstract. We measure the evolution of the galaxy Luminosity Function as a function of large-scale environment up to $z = 1.5$ from the VIMOS-VLT Deep Survey (VVDS) first epoch data. The 3D galaxy density field is reconstructed using a gaussian filter of smoothing length $5h^{-1}$ Mpc and a sample of 6582 galaxies with $17.5 \leq I_{AB} \leq 24$ and measured spectroscopic redshifts. We split the sample in four redshift bins up to $z = 1.5$ and in under-dense and over-dense environments according to the average density contrast $\delta = 0$. There is a strong dependence of the Luminosity Function (LF) with large-scale environment up to $z = 1.2$: the LF shape is observed to have a steeper slope in under-dense environments. We find $\alpha = -1.32 \pm 0.07, -1.35 \pm 0.10, -1.42 \pm 0.18$ in under-dense environments and $\alpha = -1.08 \pm 0.05, -1.06 \pm 0.06, -1.22 \pm 0.12$ in over-dense environments in the redshift bins $z = [0.25 - 0.6], [0.6 - 0.9], [0.9 - 1.2]$, respectively using a best-fit Schechter luminosity function. We find a continuous brightening of $\Delta M^* \sim 0.6$ mag from $z = 0.25$ to $z = 1.5$ both in under-dense and over-dense environments. The rest-frame B-band luminosity density continuously increases in under-dense environments from $z = 0.25$ to $z = 1.5$ whereas its evolution in over-dense environments presents a peak at $z \sim 0.9$. We interpret the peak by a complex interplay between the decrease of the star formation rate and the increasing fraction of galaxies at $\delta > 0$ due to hierarchical growth of structures. As the environmental dependency of the LF shape is already present at least up to $z = 1.2$, we therefore conclude that either the shape of the LF is imprinted very early on in the life of the Universe, a 'nature' process, or that 'nurture' physical processes shaping up environment relation have already been efficient earlier than a look-back time corresponding to 30% of the current age of the Universe.

Key words. cosmology: observations - galaxies: evolution - galaxies: luminosity function - methods: statistical

1. Introduction

Environmental effects are expected to play a key role in galaxy formation and evolution. A tight morphology-density relationship between galaxy morphology and local environment has been firmly established in clusters of galaxies, showing a strong decrease of the spiral population in the densest environments to the benefit of early-type galaxies (e.g. Dressler 1980). In the last few years, environmental effects have been systematically investigated in less extreme density regimes. In particular the Sloan Digital Sky Survey (SDSS; York et al. 2000) and the 2dF Galaxy Redshift Survey (2dFGRS; Colless et al. 2001) have allowed a complete census of the large-scale galactic environment in the local universe. At $z \sim 0.1$ and over a wide range of local galaxy densities, a strong dependency of galaxy properties with environment is observed; it includes a systematic decrease of the star formation rate towards over-dense regions (e.g. Kauffmann et al. 2004, Gómez et al. 2003) and a larger population of red galaxies in over-dense regions (Balogh et al. 2004).

Particular attention has also been devoted to investigate eventual environmental imprints on the galaxy Luminosity Function (LF). Environmental studies using small local redshift samples have provided evidence that the LF in dense environments shows a brighter M^* for groups of galaxies with increasing richness, whereas the slope does not change significantly from the field to groups (Marinoni et al. 1999, Ramella et al. 1999). The analysis based on the large SDSS and 2dFGRS surveys has confirmed this picture. For example, at $0.05 < z < 0.13$, Croton et al. (2005) find that the LF is sensitive to the large-scale environment with a top-hat smoothing length at $8h^{-1}$Mpc. They show that the galaxy LF brightens continuously from voids to clusters with no significant variation of the LF slope. Studies dedicated to specific environments go in the same direction: Hoyle et al. (2005) find a fading of the LF in voids compared to field galaxies in the SDSS; De Propris et al. (2002) find a brightening of the LF with a sample of 60 clusters in the 2dFGRS. These measurements provide a highly constrained local benchmark against which to compare environmental studies at higher redshift.

The various physical and astrophysical mechanisms which are likely to imprint an environmental dependency on galaxy properties may be classified as 'nurture' or 'nature' processes. The first are expected to be active over most of the life of a galaxy, whereas 'nature' processes would imprint an environmental dependency in some galaxy properties early on in the galaxy evolution history (see e.g. Kauffmann et al. 2004). We may discriminate inner galaxy properties from those which might be sensitive to external environments, and progress toward a better understanding of whether the dependence on environment was established early on or developed gradually as a function of time, by directly tracking the evolution of the relationship between galaxies and their surrounding environment across different cosmic epochs.

In this paper we are analysing the dependency of the galaxy luminosity function on environment up to a redshift z=1.5 from 6582 galaxies with spectroscopic redshifts in the VIMOS-VLT Deep Survey (VVDS; Le Fèvre et al. 2005). We have reconstructed the 3D density field up to $z = 1.5$ using a gaussian filter with a smoothing scale of $5h^{-1}$ Mpc in Cucciati et al. (2006). Here we investigate the dependency of the luminosity function on the large-scale environment from $z = 0.25$ to $z = 1.5$. This paper is organized as follows: we describe the data in §2, the environmental estimator in §3 and the method to compute the LF in §4. In §5 we present our results on the dependency of the LF and luminosity density on environment through cosmic time. Results are discussed in §6 and a summary is presented in §7. We adopt a flat, vacuum dominated, cosmology ($\Omega_m = 0.3$, $\Omega_\Lambda = 0.7$) and we define $h = H_0/100$ km s^{-1} Mpc^{-1}. Magnitudes are given in the AB system.

2. Data description

We use the first epoch VVDS deep sample covering 1750 arcmin^2 over the VVDS-0226-04 field (Le Fèvre et al. 2005). The spectroscopic targets are purely magnitude selected with $17.5 \le I_{AB} \le 24.0$. The sample consists of 6582 galaxies, 623 stars and 62 QSOs with reliable spectroscopic measurements (confidence level from 80 to 100%), 1439 objects with an uncertain redshift measurement (confidence level of $\sim 55\%$) and 690 objects with no spectroscopic identification. In this paper we only consider galaxies with a redshift measurement confidence level higher than 80%. The median redshift of the sample is 0.76 about with a 1σ accuracy of the redshift measurements estimated to be $dz \sim 0.0009$.

Deep multi-color images cover the entire area targeted in spectroscopy. B, V, R, I photometry was acquired with the wide-field 12K mosaic camera at the CFHT (McCracken et al. 2003; Le Fèvre et al. 2004), u^*, g', r', i', z' photometry from the Canada-France-Hawaii Legacy Survey (*www.cfht.hawaii.edu/Science/CFHLS*). The apparent magnitudes are Kron-like elliptical aperture magnitudes (Kron 1980) which have been corrected for galactic extinction from dust map images (Schlegel et al. 1998).

3. Large-scale environment: local galaxy density

We briefly summarize the method detailed in Cucciati et al. (2006) to provide a quantitative measurement of the large-scale environment.

The average density $< \rho >$ is estimated in a redshift slice with a depth of $800h^{-1}$Mpc centered on the galaxy

i. We use a gaussian smoothing method to dilute the observed point-like spatial distribution with R_S being the typical smoothing length. A local density contrast δ_i with respect to the average density $< \rho >$ is associated to each galaxy i:

$$\delta_i(R_S) = \frac{\rho_i(R_S) - <\rho>}{<\rho>}. \quad (1)$$

Each galaxy j contributes to the local density ρ_i according to:

$$\rho(r_i, R_S) = \sum_{j \neq i} \frac{w_j}{S_j} \frac{1}{(2\pi R_S^2)^{3/2}} e^{-\frac{(r_i - r_j)^2}{2R_S^2}}, \quad (2)$$

where r is the distance between the galaxies i and j, w_j is the weight associated to the galaxy j to correct for the spectroscopic incompleteness and S_j is the selection function of a flux-limited sample. Based on numerical simulations which mimic the VVDS survey, Cucciati et al. (2006) show that $R_S = 5h^{-1}$Mpc is the smallest smoothing length for which the density contrast is well recovered given the VVDS survey strategy and redshift sampling rate. In the following we use $R_S = 5h^{-1}$Mpc and the threshold $\delta = 0$ to separate under- and over-dense regions.

## 4. Procedure to compute the Luminosity Function

We derive the LF using the Algorithm for Luminosity Function (ALF) described in Appendix A of Ilbert et al. (2005). We measure k-corrections from a procedure of template fitting on the multi-color data. We derive the rest-frame luminosity at λ from the apparent magnitude observed at $\lambda \times (1 + z)$ to minimize k-correction uncertainties. Galaxies with different spectral type are not visible up to the same faint absolute magnitude limit due to the type dependency of the k-correction. This may strongly bias the LF estimate (see Ilbert et al. 2004). We therefore restrict our estimate to the absolute magnitude range complete in term of spectral type. We present results obtained on the basis of the STY (Sandage et al. 1979) and $1/V_{\max}$ (Schmidt 1968) LF estimators. For each estimator we introduce a statistical weight function of apparent magnitude and redshift that corrects for sources not observed (*Target Sampling Rate*) and for which the spectroscopic measurement failed (*Spectroscopic Success Rate*) (see Ilbert et al. 2005). The principle of the STY is to determine the Schechter parameters which maximize the likelihood to observe a given galaxy sample. This estimator allows us to describe the LF using the three parameters α, M^* and ϕ^*, and quantitatively describe the LF evolution. The $1/V_{\max}$ is complementary since this non-parametric method does not presuppose any functional form for the LF. Note that for both estimators, we are not considering the volume associated to a specific environment as done by Croton et al. (2005) but the whole volume surveyed in the given redshift bin.

5. The environment dependent Luminosity Function and Luminosity Density

We split the sample in four redshift slices from $z = 0.25$ to 1.5 and in two large-scale environment classes according to the density contrast threshold $\delta = 0$. The left panels of Fig. 1 show the resulting LFs for under- and over-dense environments. We find a clear dependence of the LF on galactic environment up to $z = 1.2$. From the non-parametric $1/V_{\max}$ estimator, we observe an excess of bright galaxies in over-dense environments compared to the luminosity distribution of galaxies in low-density regions which exhibits a larger number of faint galaxies.

We investigate this environmental dependency more quantitatively using the STY best-fitting parameters. The right panels of Fig. 1 show the STY best-fitting parameters with their 68% and 90% error contours. The best-fitting parameters are listed in Table 1. We find that the LF shape depends strongly on the large-scale environment: the differences between the $\alpha - M^*$ best-fitting values in over-dense and under-dense environments are significant at more than 90% confidence level in all the redshift bins up to $z = 1.2$. We find that the best-fitting values of the LF slope are systematically steeper in under-dense environments. We measure a difference in the slope of the LF in under-dense versus over-dense environments of $\Delta\alpha = 0.28 \pm 0.09$, 0.29 ± 0.12, 0.20 ± 0.22 in the redshift bins $z = [0.25 - 0.6]$, $[0.6 - 0.9]$, $[0.9 - 1.2]$, respectively. These differences are significant at 3σ, 2σ and 1σ, respectively. In the redshift bin $z = [1.2 - 1.5]$, the $\alpha - M^*$ parameters are too weakly constrained to conclude on a variation of α. In the redshift bin $z = 1.2 - 1.5$ the environmental dependency seems to be diminishing, but this might be a result of missing faint and red galaxies due to the VVDS selection function (see Marinoni et al. 2005, Cucciati et al. 2006). Since error contours are mostly degenerated along the magnitude axis, we observe no significant difference in M^* between under-dense and over-dense environment over the redshits range $z = 0.25 - 1.5$. According to the 90% confidence contours, we conclude that the difference in M^* between under- and over-dense environments can not be greater than ~ 1 mag, ~ 0.8 mag and ~ 1 mag at $z = 0.25 - 0.6$, $z = 0.6 - 0.9$ and $z = 0.9 - 1.2$, respectively.

Making the assumption that the LF shape (M^* and α) for a given type is universal and does not depend on the environment, a change in the relative fraction of each type as a function of the environment could change the global LF shape. The large number of galaxies at $z = 0.6 - 0.9$ in the VVDS sample allows us to measure the LF per type and environment simultaneously to test whether this assumption is correct. We split the sample at $z = 0.6 - 0.9$ in red $M_U - M_V > 1.5$ and blue $M_U - M_V < 1.5$ galaxies, which corresponds roughly to the valley in the color bimodality of the VVDS data (Franzetti et al. 2006). Figure 2 shows the shape of the LF for red and blue galaxies in under- and over-dense environments. Independantly of the spectral type, the LF slope is steeper in under-dense environments.
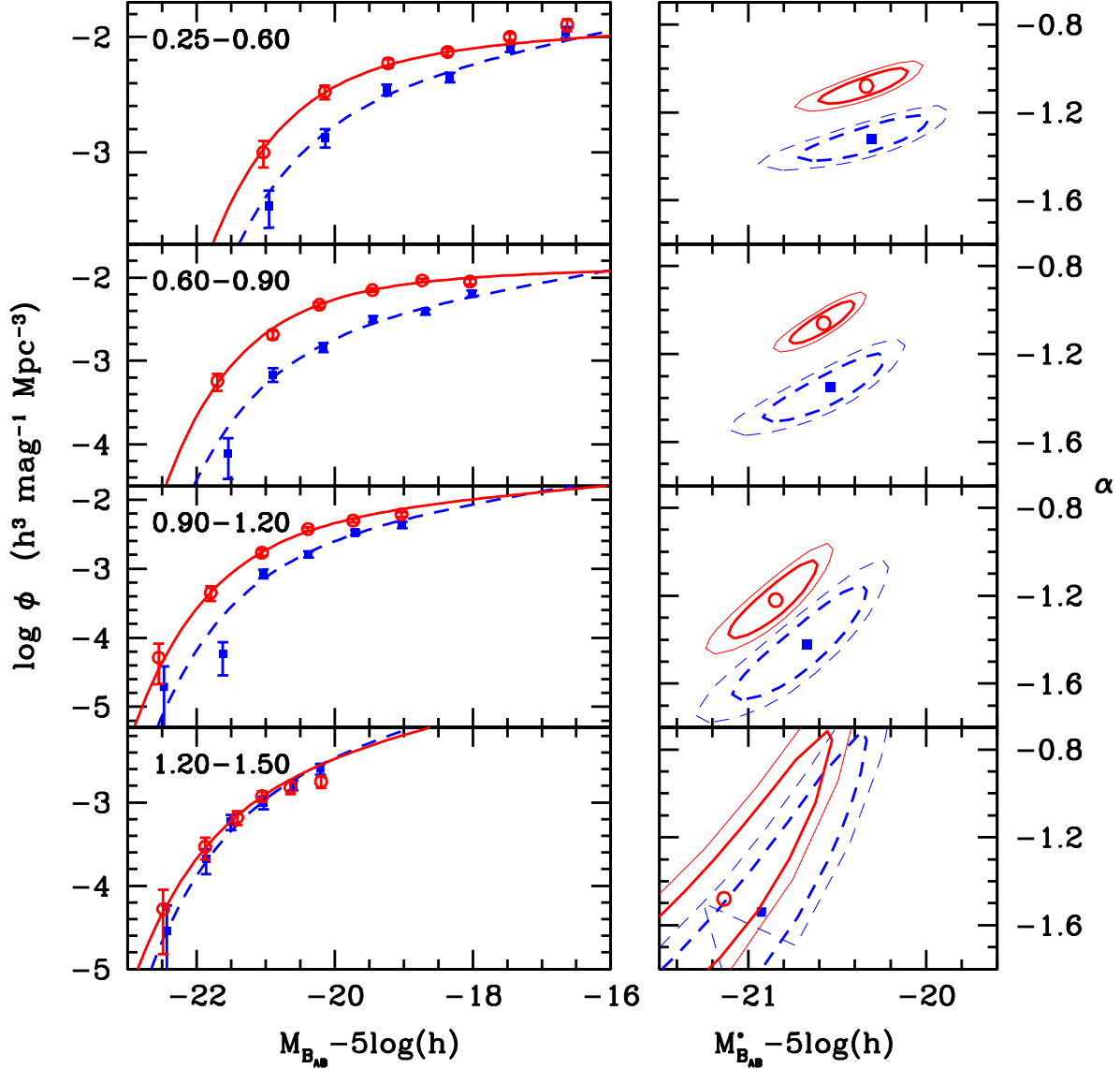
Fig. 1. Left panels: B-band LF for under-dense (blue solid squares and dashed lines) and over-dense environment (red open circles and solid lines) from $z = 0.25 - 0.6$ (top panel) up to $z = 1.2 - 1.5$ (bottom panel). The lines correspond to the best-fitting Schechter functions obtained with the STY estimator. The points correspond to the non-parametric estimate obtained with the $1/V_{\max}$ estimator. Right panels: the corresponding 68% (thick lines) and 90% (thin lines) error contours obtained with the STY estimator.

Therefore, the excess of red galaxies in over-dense environment shown in Cucciati et al. (2006) partially explains the environmental dependency of the global LF shape since we find that even the type-specific LF significantly depends on environment.

We measure the evolution of the luminosity density ρ_L in the rest-frame B band. ρ_L is directly derived from $\rho_L = \int_0^{+\infty} L\, \Phi(L)\, dL$ and we use the Schechter parameters listed in Table 1 to express $\Phi(L)$. Error bars are based on the extreme values of ρ_L calculated at each point of the $\alpha - M^*$ 1σ error contour. Fig. 3 shows the evolution of the luminosity density ρ_L as a function of redshift in both environments. In under-dense environment, we find

a continuous increase of ρ_L from $z = 0.25 - 0.6$ up to $z = 1.2 - 1.5$ by a factor 2.6. The LD evolves differently in over-dense environment: ρ_L increases between $z = 0.25 - 0.9$ then decreases or flattens at larger redshifts to become lower or equivalent to the LD in under-dense environment. An increase of the LD at the same rate than between $z = 0.25$ and $z = 0.9$ is excluded at more than 3σ. Tresse et al. (2006, in preparation) show that the uncertainty on the slope is the main source of uncertainty on ρ_L at high redshift. Since the error contours at $z = 1.2 - 1.5$ reach $\alpha < -2$, the contribution of the faint galaxies to the LD is not constrained. However, the measurements of ρ_L in the bin $z = 1.2 - 1.5$ give a good indication of

Environment	z-bin	N	α	$M^*_{B_{AB}} - 5log(h)$	Φ^* $(10^{-3}h^3Mpc^{-3})$	$\log \rho_L(B)$ $(WHz^{-1}Mpc^{-3})$
under-dense	0.25-0.60	643	$-1.32^{+0.07}_{-0.07}$	$-20.31^{+0.22}_{-0.24}$	$3.59^{+0.92}_{-0.82}$	$19.302^{+0.073}_{-0.051}$
	0.60-0.90	641	$-1.35^{+0.10}_{-0.10}$	$-20.54^{+0.21}_{-0.22}$	$3.07^{+0.87}_{-0.78}$	$19.347^{+0.069}_{-0.045}$
	0.90-1.20	471	$-1.42^{+0.18}_{-0.18}$	$-20.67^{+0.23}_{-0.25}$	$3.60^{+1.31}_{-1.14}$	$19.511^{+0.256}_{-0.094}$
	1.20-1.50	193	$-1.54^{+0.54}_{-0.55}$	$-20.93^{+0.42}_{-0.52}$	$3.58^{+2.59}_{-2.38}$	$19.716^{+23.833}_{-0.338}$
over-dense	0.25-0.60	924	$-1.08^{+0.05}_{-0.05}$	$-20.33^{+0.15}_{-0.16}$	$8.20^{+1.24}_{-1.17}$	$19.571^{+0.059}_{-0.046}$
	0.60-0.90	1440	$-1.06^{+0.06}_{-0.06}$	$-20.57^{+0.12}_{-0.12}$	$10.40^{+1.32}_{-1.28}$	$19.764^{+0.030}_{-0.026}$
	0.90-1.20	820	$-1.22^{+0.12}_{-0.12}$	$-20.84^{+0.16}_{-0.16}$	$6.63^{+1.38}_{-1.30}$	$19.735^{+0.067}_{-0.041}$
	1.20-1.50	194	$-1.48^{+0.50}_{-0.51}$	$-21.13^{+0.43}_{-0.53}$	$3.12^{+2.27}_{-2.06}$	$19.683^{+23.798}_{-0.271}$

Table 1. Schechter parameters and associated one sigma errors ($2\Delta ln\mathcal{L} = 1$) for the rest-frame B-band LF estimated with the STY. Parameters are given for under-dense and over-dense environments.

the LD expected for a "reasonable" slope $\alpha \sim -1.5$ (e.g. $\alpha = -1.44$ at $z = 0.7 - 1$ for Poli et al. 2003, $\alpha = -1.6$ at $z \sim 3$ for Steidel et al. 1999). At $z = 1.2 - 1.5$, the decrease of the LD is not constrained statistically since α is not constrained. However, the slope $\alpha = -1.48$ used at $z = 1.2 - 1.5$ is steeper by $\Delta\alpha = 0.26$ and $\Delta\alpha = 0.42$ than the slope measured at $z = 0.6 - 0.9$ and $z = 0.9 - 1.2$. Therefore, using a simple continuity argument for the slope between $z = 0.9 - 1.2$ and $z = 1.2 - 1.5$, we do not expect an increase of the LD at $z > 1.2$.

If we relate the observed evolution of the LD to the evolution of the Schechter parameters, we find that the continuous increase of ρ_L in under-dense regions is driven by a continuous brightening of M^*, with $\Delta M^*_B \sim 0.6$ mag between $z = 0.25$ and $z = 1.5$. We observe a similar brightening in over-dense environment with $\Delta M^*_B \sim 0.8$ mag. The strong decrease of ϕ^* in over-dense environment compensate the brightening of $M*$ and explains the non-monotonic behavior of the LD observed at $z \sim 0.9$.

6. Discussion

We have found that the shape of the luminosity function shows a significant dependency on the galaxy density contrast, and hence on the environment, up to a redshift at least $z = 1.2$. We find that the values of the LF slope are systematically steeper by $\Delta\alpha \sim 0.2 - 0.3$ in under-dense environments. We therefore detect at these high redshifts an environmental dependency on the slope whereas this dependency is observed only on M^* in the local Universe (eg. Marinoni et al. 1999, Ramella et al. 1999, De Propris et al. 2002, Croton et al. 2005). Local surveys at $z \sim 0.1$ find a global LF slope largely insensitive to the large-scale environment, which is explained in terms of a steepening of the LF slope for early type galaxies in over-dense regions (Croton et al. 2005). At high redshifts $z = 0.6 - 0.9$, we show that the LF of the red galaxy population, instead, shows the opposite trend with a steepening of the slope toward under-dense regions (Fig. 2). Our results are therefore suggestive of an increase of the population of faint red objects in high density environments as a function of cosmic time, consistent with the evolution of the color-environment relationship observed

by Cucciati et al. (2006). At variance with our findings on the slope α, we find that at redshifts up to $z \sim 1.5$, M^* is not significantly different in under- and over-dense environments, but our data cannot exclude variations of a few tens of a magnitude compatible with what has been found at low redshifts (e.g. an increase of M^* of $\Delta M^* = 0.3$ brighter in cluster environments than in the field De Propris et al. , 2002).

At $z \sim 1$ the luminosity distribution of galaxies that inhabit low-density regions is observed to contain a large number of faint galaxies, while the brighter galaxies are preferentially populating high-density regions. The global trend for an excess of bright galaxies in over-dense regions as shown in the local Universe (Kauffmann et al. 2004, Gómez et al. 2003, Croton et al. 2005) is therefore already present at $z \simeq 1$. This result is consistent with the VVDS luminosity-dependant clustering results (Pollo et al. 2006) and results from Bundy et al. (2006). The mass function of dark matter halos is expected to show a dependence on the large-scale environment, as predicted using an extension of the Press-Schechter formalism and confirmed in N-body cold dark matter simulations (e.g Mo & White 1996, Lemson & Kauffmann 1999). It is predicted that dark matter halos in over-dense regions should be more biased toward high masses than those forming in lower density regions. Our result therefore does not rule out that massive galaxies are build up from merging but rather implies that merging should have been already very efficient at $z > 1$.

Using the LFs, we can directly compare the relative light emissivity in under- and over-dense regions. We observe a continuous decrease of the Luminosity Density (LD) in under-dense environments from $z = 1.5$ up to $z = 0.25$, by a factor 2.6, while the LD evolution in over-dense environments presents a peak at $z \sim 0.9$. The continuous decrease of the LD in under-dense environments from $z = 1.5$ up to $z = 0.25$ is induced by the continuous fading of M^* with cosmic time. Galaxies in under-dense environments are expected to be located in more isolated small size halos (Mo et al. 2004) and should therefore evolve mainly with a passive consumption of the internal gas present in their halos. The continuous decrease
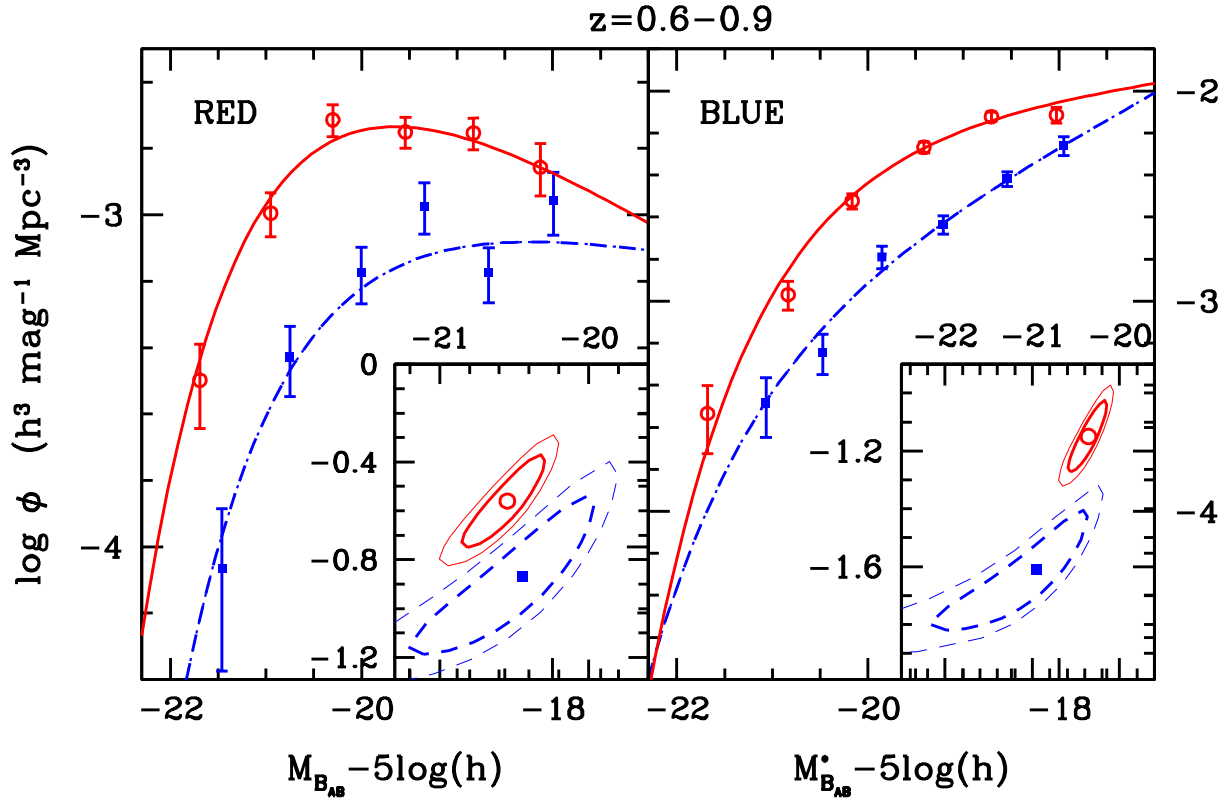
Fig. 2. B-band LF for under-dense (blue solid squares and dashed lines) and over-dense environment (red open circles and solid lines) at $z = 0.6 - 0.9$ for red (left panel) and blue galaxies (right panel). Symbols are the same as in Fig. 1.
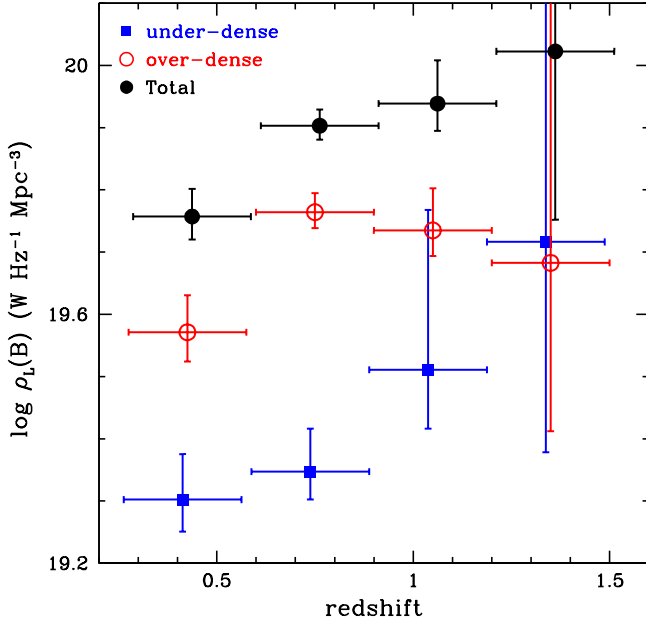
of the LD in under-dense environments observed in our data could then be due to a continuous decrease of the star formation rate in these more isolated systems. The continuous fading of M^* in over-dense environment from $z = 1.5$ to $z = 0.25$ should also lead to a continuous decrease of the LD in over-dense environment. However, an increase of ϕ^* in over-dense environments with cosmic time in effect compensates for this fading, and instead is producing an increase of the LD between $z = 1.5$ and $z = 0.9$. A relative change in the number of galaxies present above and below $\delta = 0$ could therefore explain the observed peak in the LD for the over-dense regions. In the context of the standard hierarchical scenario, the constant infalling of small-size halos (which preferentially host faint galaxies) into larger dark matter structures could explain an increase of galaxies in over-dense region. Stated differently, since galaxies become more clustered with cosmic time (e.g. Le Fèvre et al. 2005b), the relative fraction of galaxies in over-dense region increases with cosmic time. A complex interplay between the star formation rate decreasing on the one hand and the hierarchical growth of large-scale structures on the other hand could explain the peak in the LD evolution at $z \sim 0.9$. Mechanisms like strangulation resulting from the removal of the gas reservoir in larger size halos (e.g. Balogh et al. 2000) or gas stripping by the hot interstellar medium (Gunn & Gott 1972) could also play a significant role in quenching the star formation

in infalling galaxies, explaining the increasing number of faint red galaxies with cosmic time.

7. Summary

We have measured the evolution of the galaxy Luminosity Function as a function of large-scale environment up to $z = 1.5$ from the VIMOS-VLT Deep Survey (VVDS) first epoch data. The 3D galaxy density field is reconstructed using a gaussian filter of smoothing length $5h^{-1}$ Mpc and a sample of 6582 galaxies with $17.5 \leq I_{AB} \leq 24$ and measured spectroscopic redshifts. We split the sample in four redshift bins up to $z = 1.5$ and classify galaxies depending on whether they are located in under-dense or over-dense environments relative to the average density contrast $\delta = 0$. We compute the LF and LD for each of these subsamples using our dedicated tool ALF.

We find that the LF shape, characterized with the Schechter parameters $\alpha - M^*$, depends strongly on the large-scale environment from $z = 0.25$ up to $z = 1.2$: the differences between the $\alpha - M^*$ best-fitting values in over-dense and under-dense environments are significant at more than 90% confidence level in all the redshift bins up to $z = 1.2$. We therefore conclude that either the shape of the LF is imprinted very early on in the life of the Universe, a 'nature' process, or that 'nurture' physical processes shaping up the environment relation have already been efficient earlier than a look-back time corresponding to 30% of the current age of the Universe.

Fig. 3. Evolution of the Luminosity Density ρ_L measured in the B band as a function of redshift. Open red points refer to the over-dense environment, solid blue squares to the under-dense environment and solid black circles to the total sample.

The LF shape is observed to have a steeper slope in under-dense environments. We find $\alpha = -1.32 \pm 0.07, -1.35 \pm 0.10, -1.42 \pm 0.18$ in under-dense environment and $\alpha = -1.08 \pm 0.05, -1.06 \pm 0.06, -1.22 \pm 0.12$ in over-dense environment in the redshift bins $z = [0.25-0.6]$, $[0.6-0.9]$, $[0.9-1.2]$, respectively using a best-fit Schechter luminosity function. At variance, local measurements at $z \sim 0.1$ (e.g. Croton et al. 2005) do not find any dependency of the LF slope on the environment. We tentatively interpret this change as an increase of the density of faint red galaxies in over-dense environment along cosmic time.

Finally, we measure the evolution of the luminosity density ρ_L in the rest-frame B band. In under-dense environments, we find a continuous increase of ρ_L from $z = 0.25-0.6$ up to $z = 1.2-1.5$ by a factor 2.6, driven by a continuous brightening of $\Delta M^* \sim 0.6$ mag from $z = 0.25$ to $z = 1.5$. This could be the result of a passive evolution of the galaxies present in more isolated small size halos. The LD evolves differently in over-dense environment: ρ_L increases between $z = 0.25 - 0.9$ then decreases or flattens at larger redshifts. We interpret the peak at $z = 0.9$ by a complex interplay between the decrease of the star formation rate and the increasing fraction of galaxies in over-dense environment due to the hierarchical growth of structures.

References

Balogh M.L., Navarro J.F. & Morris S.L., 2000, ApJ, 540, 113
Balogh M.L., Baldry I.K., Nichol R., Miller C., Bower R. & Glazebrook K., 2004, ApJL, 615, L101
Bundy K., Ellis R.S., C.J. Conselice et al., 2006, submitted to ApJ, astro-ph/0512465
Colless M., Dalton G., Maddox S. et al., 2001, MNRAS, 328, 1039
Croton D.J., Gaztaaga E., Baugh C.M. et al., 2005, MNRAS, 356, 1155
Cucciati O. et al., in preparation, 2006
De Propris R., Colless M., Driver S.P. et al., 2002, MNRAS, 329, 87
Dressler A., 1980, ApJ, 236, 351
Franzetti P. et al., 2006, in preparation
Gómez P.L., Nichol R.C., Miller C.J. et al. 2003, ApJ, 584, 210
Gunn J.E. & Gott J.R.I., 1972, ApJ, 176, 1
Hoyle F., Rojas R.R., Vogeley M.S., Brinkmann J., submitted to ApJ, astro-ph/0309728
Ilbert O., Tresse L., Arnouts S. et al., 2004, MNRAS, 351, 541
Ilbert O., Tresse L., Zucca E. et al., 2005, A&A, 439, 863
Kauffmann G., White S.D.M., Heckman T.M. et al., 2004, MNRAS, 353, 713
Kodama T., Yamada T., Akiyama M. et al., 2004, MNRAS, 350, 1005
Kron R.G., 1980, ApJS, 43, 305
Le Fèvre O., Mellier Y., McCracken H. J. et al., 2004a, A&A, 417, 839
Le Fèvre O., Vettolani G., Garilli B. et al., 2005a, A&A, 439, 845
Le Fèvre O., Guzzo L., Meneux B. et al., 2005b, A&A, 439, 877
Lemson G. & Kauffmann G., 1999, MNRAS, 302, 111
Marinoni, C., Monaco, P., Giuricin, G., & Costantini, B., 1999, ApJ, 521, 50
Marinoni C., Le Fèvre O., Meneux B. et al., 2005, A&A, 442, 801
McCracken H.J., Radovich M., Bertin E. et al., 2003, A&A, 410, 17
Mo H.J. & White S.D.M., 1996, MNRAS, 282, 347
Mo H.J., Yang X., van den Bosch F.C., & Jing Y.P., 2004, MNRAS, 349, 205
Poli F., Giallongo E., Fontana A. et al., 2003, ApJ, 593, L1
Pollo A, Meneux B., Guzzo L. et al., 2006, A&A, submitted, (astro-ph/0512429)
Ramella, M., Zamorani, G., Zucca, E., et al. 1999, A&A, 342, 1
Sandage A., Tammann G.A., Yahil A., 1979, ApJ, 232, 352
Schmidt M., 1968, ApJ, 151, 393
Schlegel D.J., Finkbeiner D.P., & Davis M., 1998, ApJ, 500, 525

Steidel C. C., Adelberger K. L., Giavalisco M., Dickinson M.,
    Pettini M., 1999, ApJ, 519, 1
Tresse L. et al., 2006, in preparation
White S.D.M. & Frenk C.S., 1991, ApJ, 379, 52
Yee H.K.C., Hsieh B.C., Lin H. & Gladders M.D., 2005, ApJL,
    629, L77
York D.G., Adelman J., Anderson J.E. et al., 2000, AJ, 120,
    1579